C. R. Chimie 15 (2012) 911–923

Contents lists available at SciVerse ScienceDirect

Comptes Rendus Chimie

www.sciencedirect.com

Full paper/Mémoire

Synthesis, structural analysis, and thermal and spectroscopic studies of methylmalonate-containing zinc(II) complexes

Mariadel Déniz [a], Jorge Pasán [a,*], Oscar Fabelo [a,b,c], Laura Cañadillas-Delgado [a,b,c,1], Pablo Lorenzo-Luis [d], Fernando Lahoz [e], David López [e], Consuelo Yuste [f], Miguel Julve [f], Catalina Ruiz-Pérez [a,*]

[a] *Laboratorio de Rayos X y Materiales Moleculares, Departamento de Física Fundamental II, Facultad de Física, Universidad de La Laguna, Avenida Astrofísico Francisco Sánchez s/n, 38204 La Laguna (Tenerife), Spain*
[b] *Instituto de Ciencia de Materiales de Aragón, CSIC-Universidad de Zaragoza, 50009 Zaragoza, Spain*
[c] *Institut Laue-Langevin, 6, rue Jules-Horowitz, BP 156, 38042 Grenoble cedex 9, France*
[d] *Departamento de Química Inorgánica, Facultad de Química, Universidad de La Laguna, Avenida Astrofísico Francisco Sánchez s/n, 38204 La Laguna (Tenerife), Spain*
[e] *Departamento de Física Fundamental y Experimental, Electrónica y Sistemas, Facultad de Física, Universidad de La Laguna, Avenida Astrofísico Francisco Sánchez s/n, 38204 La Laguna (Tenerife), Spain*
[f] *Departament de Química Inorgànica/Instituto de Ciencia Molecular (ICMol), Facultat de Química, Universitat de València, Polígono La Coma s/n, 46980 Paterna (València), Spain*

ARTICLE INFO

Article history:
Received 5 March 2012
Accepted after revision 20 April 2012
Available online 15 June 2012

Keywords:
Carboxylate ligands
Zinc
Coordination modes
Fluorescence spectroscopy
Crystal engineering

ABSTRACT

The synthesis, crystal structure, thermal analysis and spectroscopic studies of five zinc(II) complexes of formulae $[Zn(Memal)(H_2O)]_n$ (**1**) and $[Zn_2(L)(Memal)_2(H_2O)_2]_n$ (**2**-**5**) [H_2Memal = methylmalonic acid, and L = 4,4′-bipyridine (4,4′-bpy) (**2**), 1,2-bis(4-pyridyl)ethylene (bpe) (**3**), 1,2-bis(4-pyridyl)ethane (bpa) (**4**) and 4,4′-azobispyridine (azpy) (**5**)] are presented here. The crystal structure of **1** is a three-dimensional arrangement of zinc(II) cations interconnected by methylmalonate groups adopting the μ_3-κ^2O:κO′:κO″:κO‴ *coordination mode to afford a rare (10,3)-d* **utp***-network. The structures of the compounds* **2**-**5** *are also three-dimensional and they consist of corrugated square layers of methylmalonate-bridged zinc(II) ions which are pillared by bis-monodentate 4,4′-bpy (***2***), bpe (***3***), bpa (***4***) and azpy (***5***) ligands. The Memal ligand in* **2**-**5** *adopts the* μ_3-κO:κO′:κO″:κO‴ *coordination mode. Each zinc(II) ion in* **1**-**5** *is six-coordinated with five (***1***)/four (***2***-***5***) methylmalonate-oxygen atoms, a water molecule (***1***-***5***) and a nitrogen atom from a L ligand (***2***-***5***) building distorted octahedral environments. The rod-like L co-ligands in* **2**-**5** *appear as useful tools to control the interlayer metal-metal separation, which covers the range 8.4311(5) Å (***2***) – 9.644(3) Å (***5***). The influence of the co-ligand on the fluorescence properties of this series of compounds has been analyzed and discussed by steady-state and time resolved spectroscopy on all five compounds in the solid state.*

1. Introduction

Self-assembly of metal ions and multidentate organic ligands has attracted great attention because organic spacers can alter inorganic microstructures, providing a promising route for the design of novel materials [1].

* Corresponding authors.
E-mail addresses: jpasang@ull.es (J. Pasán), caruiz@ull.es (C. Ruiz-Pérez).
[1] Present address: Centro Universitario para la Defensa, Academia General Militar, Ctra de Huesca s/n, 50090 Zaragoza, Spain.

1631-0748/$ – see front matter © 2012 Académie des sciences. Published by Elsevier Masson SAS. All rights reserved.
http://dx.doi.org/10.1016/j.crci.2012.04.007

To date, numerous coordination polymers with multifunctional frameworks have been synthesized. These hybrid inorganic-organic coordination polymers are interesting materials because of their potential applications in ion-exchange, catalysis, molecule adsorption, electric conductivities, magnetic and optical properties [2]. The architecture of the hybrid inorganic-organic networks is dependent on the geometrical preferences of the metal ions as well as on the organic linkers and blocking ligands, which exhibit remarkable diversity in their molecular structures. It deserves to be noted that in spite of the great number of results obtained and subsequent knowledge acquired, the rational design of functional materials is still at its exploratory stage and the construction of extended solids still remains unpredictable, due to many subtle interactions of reaction parameters such as temperature, time, pH value, solvent, synthetic route and stoichiometry.

Up to now, a great number of inorganic-organic hybrid coordination polymers have been synthesized based on strong covalent bonds or weak supramolecular connections such as hydrogen bonds and/or π···π interactions [3]. It has been documented that the geometries of the organic ligands have a great effect on the structural frameworks of such coordination polymers; thus, much effort has been devoted to modifying the building blocks and to controlling the assembled motifs for required products through the selection of different organic ligands. Previous studies have shown that rigid bridging ligands containing multicarboxylate groups are versatile ligands to afford moderately robust networks of variable dimensionality and porosity [4–6]. Also many compounds containing aliphatic carboxylates [deprotonated $HOOC(CH_2)_nCOOH$ derivatives] have been prepared and characterized [7]. In fact, the conformational flexibility of this type of ligands is reflected on the diversity of their connecting modes that lead to novel frameworks.

On the other hand, a rational approach to build three-dimensional structures is based on layered structural systems that can be pillared by organic linkers whose length can be modulated, aiming at fixing the interlayer separation. This strategy has been proved to be effective in the assembly of both non-covalent and covalent pillared networks [8,13a]. Rigid rod-like spacer molecules like 4,4′-bipyridine (4,4′-bpy) or 1,2-bis(4-pyridyl)ethylene (bpe) allow for some degree of control to be exerted upon the steric constrains of the assembly process and they have been used as ligands for the construction of dimensionality controlled metal-organic coordination frameworks [9–13].

Having in mind our previous results with the malonate dianion as a bridging ligand [14], and the more recent studies of copper(II) complexes with aryl/alkyl substituted malonate ligands [phenylmalonate (dianion of the phenylmalonic acid, H_2Phmal) [15] and methylmalonate (dianion of the methylmalonic acid, H_2Memal)] [13a,16], we undertook a systematic study of the structural possibilities offered by the zinc(II)/$Memal^{2-}$/L system (L being a rod-like bis-monodentate extended spacer). It is known that zinc(II) coordination complexes exhibit a wide range of structures ranging from simple chains (1D) to more complex, porous three-dimensional (3D) networks [17]. Previous attempts on complex formation between substituted malonate and zinc(II) ions yielded either mononuclear complexes using blocking ligands [18] or polynuclear malonate-bridged compounds with several co-ligands [19]. In particular, only five zinc(II) complexes of malonate/substituted malonate without coligands have been reported: three of them are polynuclear compounds of formulae $[Zn(R\text{-}mal)(H_2O)_m]_n$ [R-mal = 3-hydroxycyclobutane-1,1-dicarboxylate ($m = 2$), 2,2-dimethylmalonate ($m = 1$) and malonate ($m = 2$)] and the other two are mononuclear species of formula $[Zn(Hmal)_2(H_2O)_2]$ (H_2mal = malonic acid) [20].

The geometrical constraints caused by the insertion of a methyl group on the methylene carbon atom could induce different conformations of the resulting methylmalonate as a ligand when compared to its parent malonate group. At this respect, previous studies concerning the compounds $[Cu(Memal)(H_2O)]_n$, $[Cu_2(pyz)(Memal)_2]_n$ and $[Cu_2(4,4'\text{-bpy})(Memal)_2(H_2O)_2]_n$, (pyz = pyrazine) showed that it is possible to exert some control over these conformations using the appropriate co-ligands [13a]. This series of complexes is particularly interesting because the bis-monodentate rod-like spacer acts as a pillar of the corrugated layers of methylmalonate-bridged copper(II) ions providing, thus, a safe strategy to tune the separation between magnetic layers.

In the present work, we focus on the synthesis, structural characterization, thermal behaviour and luminescent properties of five methylmalonate-containing zinc(II) complexes of formula $[Zn(Memal)(H_2O)]_n$ (**1**) and $[Zn_2(L)(Memal)_2(H_2O)_2]_n$ (**2-5**) [L = 4,4′-bipyridine (4,4′-bpy) (**2**), 1,2-bis(4-pyridyl)ethylene (bpe) (**3**), 1,2-bis(4-pyridyl)ethane (bpa) (**4**) and 4,4′-azobispyridine (azpy) (**5**), Scheme 1]. The crystal structure of **2** was reported previously [16a] and we only refer to it here for comparative purposes. Interestingly, **1** is quite different with respect to the related copper(II) complex [13a], the zinc(II) compound exhibiting an unusual three-dimensional (10,3)-d network. Complexes **2-5** are also 3D compounds where the corrugated layers of Zn(II)-methylmalonate are pillared by the rod-like L coligands.

2. Experimental

2.1. Materials and methods

Solvents and reagents utilized in the synthesis, except 4,4′-azobispyridine, were purchased from commercial sources and used without further purification. The azpy molecule was synthesized by means of the oxidation of 4-aminopyridine by a solution of sodium hypochlorite [21]. Compound **2** was prepared as previously described [16a]. Elemental analyses (C, H, N) were performed with an EA 1108 CHNS/0 automatic analyzer. Thermal analyses were carried out on a PerkinElmer system (mod. Pyris Diamond TG/DTA, SEGAI Service of the ULL-University) under a nitrogen atmosphere (with a flow rate of 80 $cm^3\ min^{-1}$) in the temperature range 25–950 °C. The samples (ca. 20 mg) were heated in a platinum crucible at a rate of 10 °C min^{-1}. The TG curves were analyzed as the

percentage of mass loss as a function of temperature. The numbers of decomposition steps were identified using the derivative thermogravimetric curve (DTG). The DTA curves were analyzed as differential thermal analysis ($\Delta T(\mu V)$).

2.2. Preparation of the complexes

2.2.1. $[Zn(Memal)(H_2O)]_n$ (1)

Zinc(II) acetate dihydrate (1 mmol, 219 mg) was added to a warm (60 °C) aqueous solution (30 cm^3) of methylmalonic acid (1 mmol, 118 mg) under continuous stirring. After cooling, the resulting colourless clear solution was allowed to evaporate at room temperature and prismatic colourless single crystals of **1** appeared after a few days. Yield: 73%. Anal. Calc. for $C_4H_6ZnO_5$ (**1**): C, 24.09; H, 3.03. Found: C, 24.03; H, 3.08. Selected IR peaks (KBr, cm^{-1}): 3317w, 1551vs, 1389s, 1288 m, 710 m, 605 s.

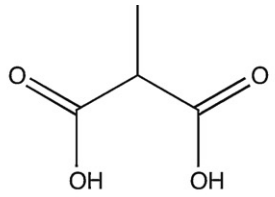

Methylmalonic acid (H_2Memal)

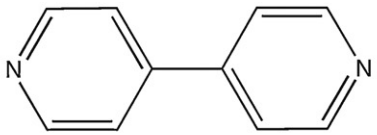

4,4'-bipyridine (4,4'-bpy)

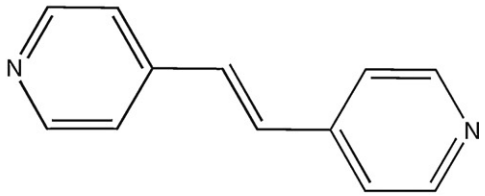

1,2-bis(4-pyridyl)ethylene (bpe)

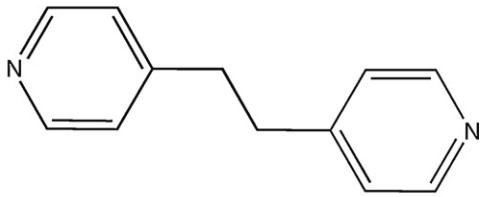

1,2-bis(4-pyridyl)ethane (bpa)

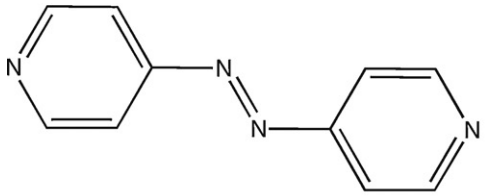

4,4'-azobispyridine (azpy)

Scheme 1.

2.2.2. $[Zn_2(L)(Memal)_2(H_2O)_2]_n$ [L = bpe (3), bpa (4) and azpy (5)]

Methylmalonic acid (0.5 mmol, 59 mg) and sodium carbonate (0.5 mmol, 53 mg) were mixed in water (5 cm^3) and the resulting clear solution was placed at the bottom of a test tube. Then, a water interphase (6 cm^3) was added and an aqueous solution (2 cm^3) of zinc(II) nitrate hexahydrate (0.5 mmol, 149 mg) was carefully added on the top. Finally, another water interphase (6 cm^3) was added and a methanolic solution (3 cm^3) of bpe (0.5 mmol, 91 mg) (**3**), bpa (0.5 mmol, 92 mg) (**4**) or azpy (0.5 mmol, 92 mg) (**5**) was carefully layered on the top of the tube. The tubes were covered with parafilm and stored at room temperature. X-ray suitable colourless needles (**3** and **4**) and prisms (**5**) were obtained after a few weeks. Yield: 81% (**3**), 76% (**4**) and 86% (**5**). Anal. Calc. for $C_{10}H_{11}ZnNO_5$ (**3**): C, 41.33 (**3**); H, 3.82 (**3**); N, 4.82 (**3**). Found: C, 41.37; H, 3.79; N, 4.85%. Anal. Calc. for $C_{10}H_{12}ZnNO_5$ (**4**): C, 41.19; H, 4.15; N, 4.80. Found: C, 41.24; H, 4.12; N, 4.82%. Anal. Calc. for $C_9H_{10}ZnN_2O_5$ (**5**): C, 38.67; H, 4.33; N, 5.01. Found: C, 38.73; H, 4.36; N, 5.06% (**5**). Selected IR peaks (KBr, cm^{-1}): 3128w, 1551vs, 1443 m, 1331s, 706 m, 544 s (**3**); 3090w, 1558vs, 1431 m, 1335s, 814 s, 544 m (**4**); 3124w, 1558vs, 1331 m, 837 m, 710 m, 563 s (**5**).

2.3. X-ray data collection and structure determination

Single crystals of **1** and **3**-**5** were mounted on a Bruker-Nonius KappaCCD diffractometer, and the crystallographic data were collected at 293(2) K by using graphite-monochromated Mo-Kα radiation (λ = 0.71073 Å). Their crystal structures were solved by direct methods and refined with the full-matrix least-squares technique on F^2 by using the SHELXS-97 and SHELXL-97 programs [22] included in the WINGX [23] software package. All non-hydrogen atoms were refined anisotropically. The aromatic rings of the azpy ligands in **5** are disordered between two positions with occupancy factors of 0.51 and 0.49. The s.o.f. was allowed to refine with the whole set of parameters. The hydrogen atoms of the Memal and L ligands in **1** and **3**-**5** were set on geometrical positions and refined with a riding model whereas those of the water molecules were found in Fourier difference maps (except in **3** where they were neither found nor set). The final geometrical calculations and the graphical manipulations were carried out with PLATON [24] and DIAMOND[2] programs. A summary of the crystallographic data and structure refinement of **1** and **3**-**5** is given in Table 1.

[2] DIAMOND 2.1d, Crystal Impact GbR, CRYSTAL IMPACT, K. Brandenburg & H. Putz GbR, Postfach 1251, 53002 Bonn, Germany, 2000.

Table 1
Crystallographic data for complexes **1** and **3**-**5**.

	1	**3**	**4**	**5**
Formula	$C_4H_6O_5Zn$	$C_{10}H_{11}O_5N\ Zn$	$C_{10}H_{12}O_5N\ Zn$	$C_9H_{10}O_5N_2Zn$
FW	199.46	290.57	291.58	291.56
Crystal system	Orthorhombic	Monoclinic	Orthorhombic	Orthorhombic
Space group	*Pna2₁*	*P2₁/n*	*P mnn*	*P mnn*
a (Å)	8.072(2)	7.0598(3)	7.582(2)	7.3390(10)
b (Å)	8.166(2)	20.8448(10)	6.863(5)	21.735(5)
c (Å)	9.1623(11)	7.4944(3)	21.039(14)	7.213(5)
β (°)	–	92.482(3)	–	–
V (Å^3)	603.9(2)	1101.84(8)	1094.8(12)	1149.3(11)
Z	4	4	4	4
μ (Mo Kα) (cm^{-1})	4.022	2.238	2.252	2.148
T (K)	293(2)	293(2)	293(2)	293(2)
ρ_{cal} (g cm^{-3})	2.194	1.752	1.769	1.685
λ (Å)	0.71073	0.71073	0.71073	0.71073
Index ranges	$-11 \le h \le 11$ $-6 \le k \le 11$ $-11 \le l \le 13$	$-9 \le h \le 7$ $-27 \le k \le 26$ $-8 \le l \le 9$	$-9 \le h \le 9$ $-8 \le k \le 5$ $-27 \le l \le 27$	$-9 \le h \le 7$ $-25 \le k \le 28$ $-9 \le l \le 7$
Indep. Reflect. (R_{int})	1782 (0.0632)	2501 (0.1073)	1319 (0.0593)	1407 (0.0852)
Flack parameter [25]	0.00(3)	–	–	–
Obs. reflect. [I > 2σ(I)]	1548	1534	965	879
Parameters	100	154	92	99
Goodness-of-fit	0.988	1.158	1.080	1.102
R [I > 2σ(I)]	0.0466	0.0856	0.0462	0.0718
R_w [I > 2σ(I)]	0.0976	0.1882	0.0819	0.0938
R (all data)	0.0559	0.1521	0.0784	0.1353
R_w (all data)	0.1029	0.2137	0.0924	0.1113

Table 2
Selected bond distances (Å) and angles (°) and intermolecular interactions (Å,°) for complex **1**.[a]

1					
Zn(1)–O(1W)	2.020(4)	O(1W)–Zn(1)–O(2)	106.51(13)	O(2)–Zn(1)–O(1a)	102.93(12)
Zn(1)–O(4)	2.044(4)	O(4)–Zn(1)–O(2)	87.74(13)	O(3b)–Zn(1)–O(1a)	88.05(14)
Zn(1)–O(2)	2.047(3)	O(1W)–Zn(1)–O(3b)	96.25(16)	O(1W)–Zn(1)–O(2a)	91.84(13)
Zn(1)–O(3b)	2.076(3)	O(4)–Zn(1)–O(3b)	171.45(15)	O(4)–Zn(1)–O(2a)	90.43(13)
Zn(1)–O(1a)	2.172(3)	O(2)–Zn(1)–O(3b)	85.68(12)	O(2)–Zn(1)–O(2a)	161.58(13)
Zn(1)–O(2a)	2.271(3)	O(1W)–Zn(1)–O(1a)	150.48(13)	O(3b)–Zn(1)–O(2a)	94.08(12)
O(1W)–Zn(1)–O(4)	90.84(16)	O(4)–Zn(1)–O(1a)	88.10(15)	O(1a)–Zn(1)–O(2a)	58.68(11)

D–H ··· A[b]	D–H (Å)	H ··· A (Å)	D ··· A (Å)	D–H ··· A (°)
O(1W)–H(1WA) ··· O(1c)	0.83(2)	1.94(2)	2.752(5)	167(5)
O(1W)–H(1WB) ··· O(3d)	0.85(2)	1.96(2)	2.782(5)	163(5)
O(1W)–H(1WB) ··· O(4d)	0.85(2)	2.59(5)	3.099(4)	120(4)

[a] Symmetry code: (a) = $x + ½, -y + ½, z$; (b) = $-x + ½, y - ½, z + ½$; (c) = $-x + 1, -y, z - ½$; (*d*) = $-x + 1, -y + 1, z - ½$.
[b] D and A stand for donor and acceptor, respectively.

Selected bonds and angles together with the hydrogen bonds are listed in Tables 2 (**1**) and 3 (**3**-**5**). Selected structural data for **2** are also included in Table 2 in order to make easier the structural comparison with **3**-**5**.

2.4. Optical measurements

Fluorescence measurements were performed in a LifeSpecII spectrometer (Edinburgh Instruments). A pulsed

Table 3
Selected bond distances (Å) and angles (°) and intermolecular interactions (Å,°) for complexes **2**-**5**.[a]

2					
Zn(1)–O(4)	2.0880(14)	O(4)–Zn(1)–O(2)	85.18(5)	O(2)–Zn(1)–O(1W)	92.20(6)
Zn(1)–O(3e)	2.1001(13)	O(3e)–Zn(1)–O(2)	87.53(5)	O(1f)–Zn(1)–O(1W)	89.70(5)
Zn(1)–O(2)	2.1013(13)	O(4)–Zn(1)–O(1f)	89.15(5)	O(4)–Zn(1)–N(1)	87.99(6)
Zn(1)–O(1f)	2.1228(13)	O(3e)–Zn(1)–O(1f)	98.00(6)	O(3e)–Zn(1)–N(1)	88.29(6)
Zn(1)–O(1W)	2.125(2)	O(2)–Zn(1)–O(1f)	174.03(5)	O(2)–Zn(1)–N(1)	91.98(6)
Zn(1)–N(1)	2.161(2)	O(4)–Zn(1)–O(1W)	90.57(6)	O(1f)–Zn(1)–N(1)	85.96(6)
O(4)–Zn(1)–O(3e)	171.69(5)	O(3e)–Zn(1)–O(1W)	93.68(6)	O(1W)–Zn(1)–N(1)	175.45(6)
3					
Zn(1)–O(4)	2.126(6)	O(2)–Zn(1)–O(4)	85.1(2)	O(2)–Zn(1)–O(1W)	90.8(2)
Zn(1)–O(3f)	2.133(6)	O(2)–Zn(1)–O(3f)	87.4(2)	O(1e)–Zn(1)–O(1W)	92.9(2)
Zn(1)–O(2)	2.074(6)	O(1e)–Zn(1)–O(4)	85.7(2)	O(4)–Zn(1)–N(1)	92.2(3)
Zn(1)–O(1e)	2.086(6)	O(1e)–Zn(1)–O(3f)	101.8(2)	O(3f)–Zn(1)–N(1)	87.5(2)
Zn(1)–O(1W)	2.135(6)	O(2)–Zn(1)–O(1e)	170.2(2)	O(2)–Zn(1)–N(1)	88.4(3)
Zn(1)–N(1)	2.158(7)	O(4)–Zn(1)–O(1W)	92.3(2)	O(1e)–Zn(1)–N(1)	88.6(3)
O(4)–Zn(1)–O(3f)	172.5(2)	O(3f)–Zn(1)–O(1W)	87.8(2)	O(1 W)–Zn(1)–N(1)	175.3(2)
4					
Zn(1)–O(2)	2.088(2)	O(2j)–Zn(1)–O(1k)	85.88(10)	O(1k)–Zn(1)–O(1W)	90.47(10)
Zn(1)–O(2j)	2.088(2)	O(2)–Zn(1)–O(1k)	171.40(10)	O(1 g)–Zn(1)–O(1W)	90.47(10)
Zn(1)–O(1k)	2.125(2)	O(2j)–Zn(1)–O(1g)	171.40(10)	O(2j)–Zn(1)–N(1)	91.90(12)
Zn(1)–O(1g)	2.125(2)	O(2)–Zn(1)–O(1g)	85.88(10)	O(2)–Zn(1)–N(1)	91.90(12)
Zn(1)–O(1W)	2.129(4)	O(1k)–Zn(1)–O(1g)	102.54(14)	O(1k)–Zn(1)–N(1)	86.88(11)
Zn(1)–N(1)	2.136(4)	O(2j)–Zn(1)–O(1W)	91.22(12)	O(1 g)–Zn(1)–N(1)	86.88(10)
O(2j)–Zn(1)–O(2)	85.66(14)	O(2)–Zn(1)–O(1W)	91.22(12)	O(1 W)–Zn(1)–N(1)	175.8(2)
5					
Zn(1)–O(2)	2.096(3)	O(2 m)–Zn(1)–O(1h)	172.16(13)	O(1 h)–Zn(1)–O(1W)	91.79(14)
Zn(1)–O(2m)	2.096(3)	O(2)–Zn(1)–O(1h)	87.75(13)	O(1n)–Zn(1)–O(1W)	91.79(14)
Zn(1)–O(1h)	2.101(3)	O(2m)–Zn(1)–O(1n)	87.75(13)	O(2 m)–Zn(1)–N(1)	90.5(2)
Zn(1)–O(1n)	2.101(3)	O(2)–Zn(1)–O(1n)	172.16(13)	O(2)–Zn(1)–N(1)	90.5(2)
Zn(1)–O(1W)	2.122(5)	O(1h)–Zn(1)–O(1n)	99.0(2)	O(1 h)–Zn(1)–N(1)	86.14(14)
Zn(1)–N(1)	2.160(6)	O(2m)–Zn(1)–O(1W)	91.9(2)	O(1n)–Zn(1)–N(1)	86.14(14)
O(2 m)–Zn(1)–O(2)	85.2(2)	O(2)–Zn(1)–O(1W)	91.9(2)	O(1 W)–Zn(1)–N(1)	176.8(2)

2				
D–H ··· A[b]	D–H (Å)	H ··· A (Å)	D ··· A (Å)	D–H ··· A (°)
O(1W)–H(1WB) ··· O(2f)	0.878(13)	1.86(2)	2.703(2)	161(3)
O(1W)–H(1WA) ··· O(4e)	0.80(3)	1.89(3)	2.665(2)	162(3)

3				
D–H ··· A[b]	D–H (Å)	H ··· A (Å)	D ··· A (Å)	D–H ··· A (°)
O(1W) ··· O(2e)	–	–	2.639(8)	–
O(1W) ··· O(4f)	–	–	2.698(8)	–

4				
D–H ··· A[b]	D–H (Å)	H ··· A (Å)	D ··· A (Å)	D–H ··· A (°)
O(1W)–H(1WA) ··· O(2g)	0.89(2)	1.83(2)	2.669(3)	156(4)

5				
D–H ··· A[b]	D–H (Å)	H ··· A (Å)	D ··· A (Å)	D–H ··· A (°)
O(1W)–H(1WA) ··· O(2h)	0.88(2)	1.82(3)	2.665(5)	159(6)

[a] Symmetry code: (e) = $x - ½, -y + ½, z - ½$; (f) = $x - ½, -y + ½, z + ½$; (g) = $-x + 3/2, y + ½, -z + 3/2$; (h) = $-x - ½, -y + ½, z + ½$; (j) = $-x + 1, y, z$; (k) = $x-½, y + ½, -z + 3/2$; (m) = $-x, y, z$; (n) = $x + ½, -y + ½, z + ½$.
[b] D and A stand for donor and acceptor, respectively.

diode laser at 405 nm was used as the excitation source. The repetition rate was fixed at 1 MHz and the temporal pulse width was around 70 ps. The average pump power was about 5 mW. In order to avoid polarization effects, a detection polarizer was set at the magic angle. The emission was collected by a convergence lens and dispersed by a low temporal dispersion monochromator. The light was detected by a multichannel plate-photomultiplier using time correlated single photon counting technique. The instrumental response function of the equipment showed a temporal width at half maximum of about 70 ps.

3. Results and discussion

3.1. Description of the structures

3.1.1. $[Zn(Memal)(H_2O)]_n$ (1)

Compound **1** crystallizes in the non-centrosymmetric orthorhombic space group $Pna2_1$ and its crystal structure

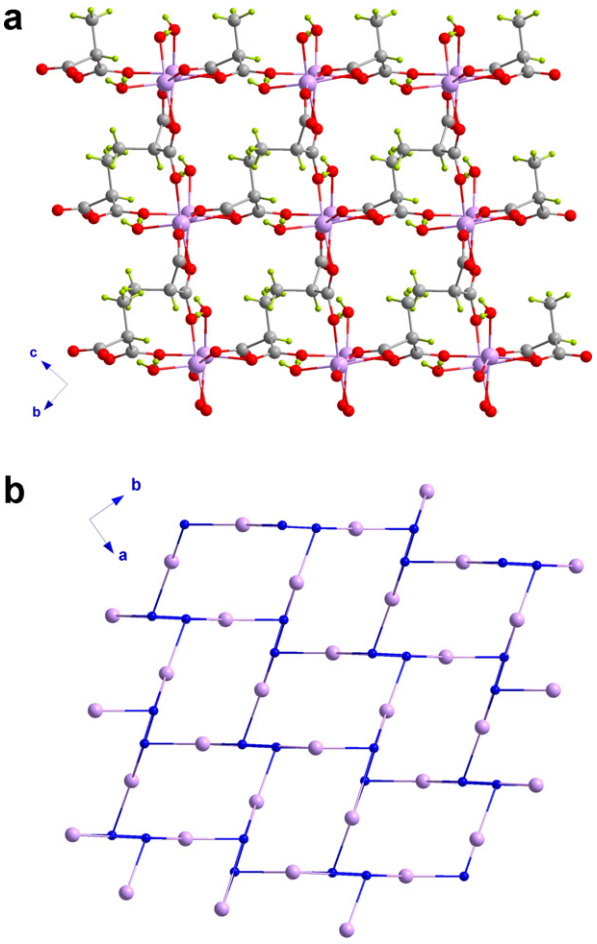

Fig. 1. a: a view of the crystal packing of **1** along the crystallographic *a* axis; b: topological view of **1** along the *c* axis showing the typical [6^3] view of the (10,3)-d **utp**-nets.

consists of a three-dimensional (10,3)-d **utp**-net [26], considering the $Memal^{2-}$ ligand and the $[Zn(H_2O)]^{2+}$ unit as the three-fold connector and node, respectively (Figs. 1 and 2). This is a rare topology and only a few metal-organic

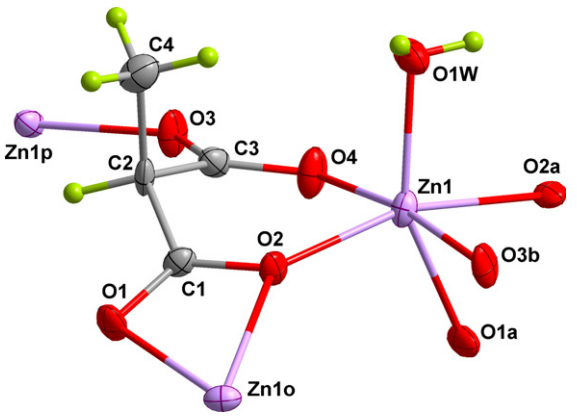

Fig. 2. View of a fragment of **1** with the numbering scheme. [symmetry code: (o) = $-x+½, y+½, z-½$; (p) = $x-½, -y+½, z$].

frameworks exhibiting this network have been reported [27,28]. Interpenetration is frequent in this type of structures [27] but the small size of the Memal group precludes this structural feature in **1**. Also, the methyl groups of the Memal ligand are arranged in a polar way along the crystallographic *c* axis, a situation that can lead the non-centrosymmetric packing of **1** [29].

The whole structure can be viewed as interwoven chains of $[Zn(Memal)]_n$ where Zn(II) ions are linked through *anti-anti* carboxylate bridges. These chains run in the [10-1] and [101] directions and are linked together through μ-oxo carboxylate bridges. The values of the separation between the Zn(II) ions through the *anti-anti* carboxylate and μ-oxo(carboxylate) bridges are 6.160(1) and 4.073(1) Å, respectively.

Each zinc(II) atom exhibits a distorted octahedral environment with four short coordination bonds [O(2), O(4), O(1w) and O(3b); b = $-x+½, y-½, z+½$] with an average distance of 2.047(4) Å, and two longer ones [O(1a) and O(2a); a = $x+½, -y+½, z$] with a mean bond distance of 2.221(3) Å. The values of the degree of compression (s/h) and twisting angle (φ) are 1.162 Å and 57.4°, respectively (s/h = 1.22 and φ = 60° for a regular octahedron) [30]. This distortion comes from the constraints of the carboxylate chelation through O(1a) and O(2a).

The methylmalonate ligand adopts the μ_3-$\kappa^2O{:}\kappa O'{:}\kappa O''{:}\kappa O'''$ coordination mode: bidentate mode towards Zn(1) through the O(2) and O(4) atoms from the two carboxylate groups [bite angle of 87.74(13)° adopting a boat conformation] together with carboxylate chelation at Zn(1o) across O(1) and O(2) [bite angle of 58.68(11)°; (o) = $-x+½, y+½, z-½$] and monodentate coordination towards Zn(1p) through O(3) [(p) = $x-½, -y+½, z$] (Fig. 2). This bridging mode is unprecedented for R-malonate complexes of transition metal ions, because the carboxylate chelation of transition metal ions is difficult due to their small ionic radii compared to those of the lanthanides where this four-member chelation is more common. The long Zn-O bond distances of the carboxylate chelation [mean value of 2.221(3) Å] and the small bite angle [58.68(11)°] induce us to consider the possibility of a monodentate coordination of this carboxylate instead of its chelation. In doing so, the Zn(II) environment can be viewed as a distorted trigonal bipyramid with a τ value of 0.65 [31]. Interestingly, the methyl group of the Memal ligand is directed parallel to the Zn–O(1w) bond (Fig. 2), allowing the *anti-anti* conformation of the carboxylate bridge. This feature is uncommon in the R-malonate complexes [13a,16,19], although it has been previously observed in the crystal structure of the compound{[Mn(Etmal)$_2$(H_2O)][Mn(H_2O)$_4$]}$_n$ (H_2Etmal = ethylmalonic acid) [16].

3.1.2. $[Zn_2(L)(Memal)_2(H_2O)_2]_n$ with L = bpe (3), bpa (4) and azpy (5)

The crystal structures of **3-5** consist of corrugated zinc(II)-methylmalonate hexagonal layers pillared through 1,2-bis(4-pyridyl)ethylene (**3**), 1,2-bis(pyridyl)ethane (**4**) and 4,4′-azobispyridine (**5**) ligands to build up a 3D network exhibiting a topology of a 3,4-binodal net with a Schläfli symbol [6^3] [$6^5 8$] **ins**-net [32] (Figs. 3 (**4**), S1

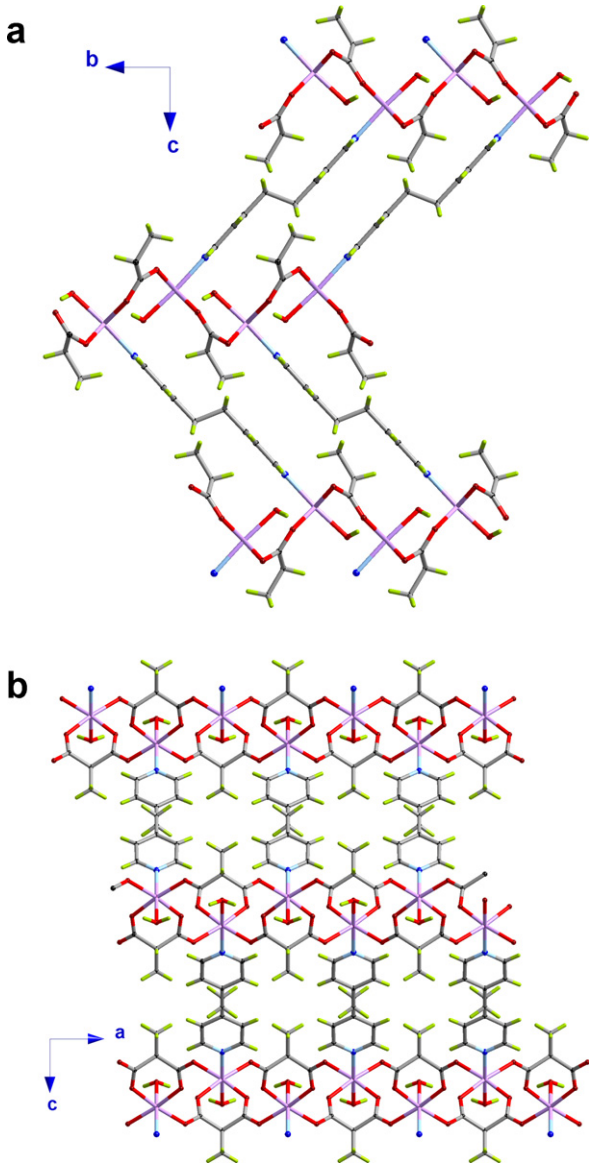

Fig. 3. View of the crystal packing of the pillared structure of **4** along the *a* (a) and *b* axes (b).

(**3**) and S2 (**5**)). The same net was observed by some of us in a previous report with L = 4,4′-bipyridine (compound **2**, Fig. S3) [16a]. This framework is formed by the pillaring of a corrugated [6^3] two-dimensional net formed by *anti-syn* carboxylate(methylmalonate) bridged Zn(II) ions through bis-monodentate rod-like spacers (L). The size of the methyl group of the methylmalonate ligand is small enough to allow the L ligands [4,4′-bpy (**2**), bpe (**3**), bpa (**4**) and azpy (**5**)] to connect the layers and they are located alternatively above and below the sheets, in a *trans* arrangement with the methyl group of the Memal ligand (Figs. 3, S1–S3 and 4). Although the pillaring ligands have aryl groups, no π-π interactions occur in these structures, the centroid-centroid distances between adjacent rings being in the range 6.8–7.3 Å [33]. However, C–H/π interactions have been found in **5** due to the delocalization of the azpy groups. The distance between the centroid of the pyridyl ring and the adjacent aryl C-H group is 2.583(1) Å. Intralayer hydrogen bonds involving the coordinated water molecule and oxygen atoms of the methylmalonate ligand occur in **2**-**5** (Table 3).

Each zinc atom exhibits a distorted octahedral environment. The values of the *s/h* and *φ* parameters of the octahedra are 1.237 and 59.20° (**2**), 1.192 and 58.66° (**3**), 1.188 and 56.94° (**4**) and 1.206 and 57.35° (**5**). Four Memal oxygen atoms, a water molecule and a nitrogen atom from a 4,4′-bpy (**2**), bpe (**3**), bpa (**4**) and azpy (**5**) ligands define the octahedral environment at the zinc atom, the Zn–N bond length being systematically longer than the Zn–O ones (Table 2).

The methylmalonate ligand in **2-5** exhibits the μ_3-κ*O*:κ*O*′:κ*O*″:κ*O*‴ coordination mode: bidentate coordination towards Zn(1) through O(2) and O(4) (**2** and **3**), O(2) and O(2j) (**4**), and O(2) and O(2m) (**5**) in a boat conformation [bite angle of 85.17(5)° (**2**), 85.09(1)° (**3**), 85.67(4)° (**4**) and 85.22(12)° (**5**)] and bis-monodentate [through O(1) to Zn(1n) and O(3) to Zn(1q) (**2** and **3**), across O(1) to Zn(1r) and O(1j) to Zn(1s) (**4**) and through O(1) to Zn(1t) and O(1m) to Zn(1u) (**5**); symmetry code: (j) = –*x* + 1, *y*, *z*; (m) = -*x*, *y*, *z*; (n) = *x* + ½, –*y* + ½, *z* + ½; (q) = *x* + ½, –*y* + ½, *z*–½; (r) = –*x* + 3/2, *y*–½, –*z* + 3/2; (s) = –*x* + ½, *y*–½, –*z* + 3/2; (t) = –*x*–½, –*y* + ½, *z*–½; (u) = –*x* + ½, –*y* + ½, *z*–½]. This coordination makes the Memal a three-fold connector. In addition, the methyl group of the Memal ligand is located in the mean plane of the six-membered chelate contrary to what was observed for **1** where it was perpendicular to it, this structural feature causing the corrugation of the square Memal-bridged zinc(II) layers in **2**-**5**.

The pyridyl rings of the 4,4′-bpy ligand in **2** are coplanar because there is an inversion centre located at the middle of the central C–C bond. There is also an inversion centre at the middle of the middle point of the ethylene (**3**), ethane (**4**), and azo (**5**) groups, but the pyridyl rings are parallel, although not coplanar, with a separation between the two aryl planes of 0.677(1) (**3**), 1.4677(5) (**4**) and 0.569(11) Å (**5**). The aryl groups of the ligand occupy two possible positions in **2** and **5**, with occupancy parameters of 0.28 and 0.72, and 0.51 and 0.49, respectively, and a dihedral angle between the pyridyl rings of 38.1(5)° (**2**) and 90° (**5**).

The rod-like L spacers connect two zinc atoms from adjacent layers, the separation between them being dependent on the ligand length. The values of the distance between Zn(II) cations through these spacers are 11.4140(5) Å (**2**), 13.6128(4) (**3**), 13.499(7) (**4**) and 13.318(5) Å (**5**). It deserves to be noted that these values are longer than the shortest interlayer Zn···Zn separation [8.4311(5) (**2**), 9.4357(2) (**3**), 9.490(6) (**4**) and 9.644(3) Å (**5**)] because of the corrugation of the layers and the non-parallel alignment of the bridging ligands along the stacking direction of the layers. Thus, the normal of the layers form an angle with the rigid spacers of 45.11(7)° (**2**), 48.77(3)° (**3**), 49.54(3)° (**4**) and 45.93(4)° (**5**). Finally, the values of the intralayer zinc···zinc separations through the *anti-syn* carboxylate bridges are in the range

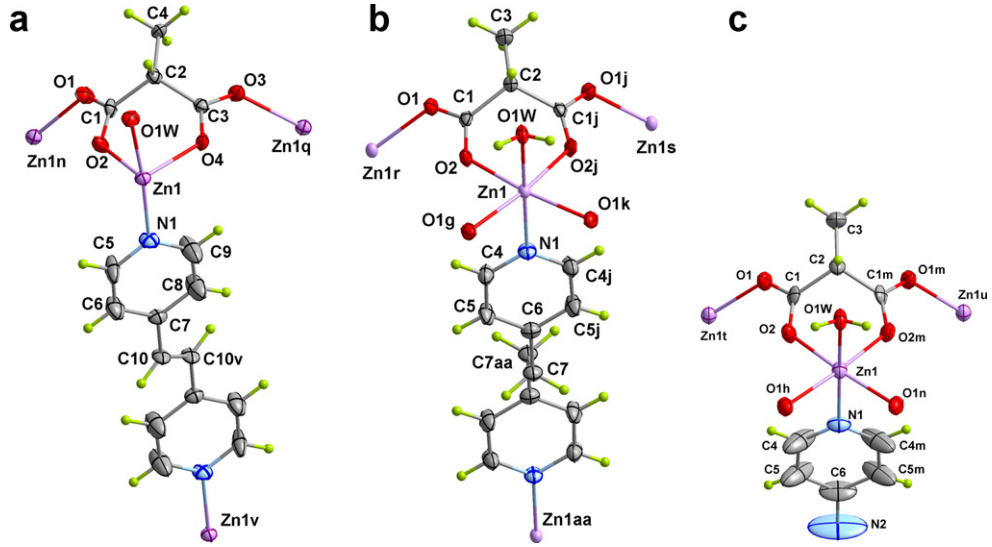

Fig. 4. View of a fragment of the structures of **3**-**5** along with the numbering scheme (symmetry codes: v = –*x* + 2, –*y* + 1, –*z* + 1; aa = *x*, –*y*, –*z* + 1).

5.291(4)–5.439(4) (**2**), 5.494(1)–5.282(1) (**3**), 5.363(2) (**4**) and 5.353(3) Å (**5**).

3.2. Structural overview of the R-mal/Zn(II) complexes

A survey of the literature shows that the crystal structure of five different R-malonate/Zn(II) complexes with water molecules as the only co-ligands have been previously reported [20] (CSD refcodes are listed in ref. [19]). The crystal structures of these compounds can be grouped in three different families. The first one are the compounds QQQFRG (**6**) and ZNHMAL (**7**) compounds of formula $Zn(Hmal)_2(H_2O)_2$ (H_2mal = malonic acid) crystallizing in the *Pbam* and $P2_1/c$ space groups, respectively. They are formed by mononuclear entities built up from two partially protonated malonate ligands chelating the zinc(II) metal ions. Two *trans* water molecules fill the two remaining sites of the somewhat distorted octahedral environment of the zinc(II) ion. These monomers are kept together through an extensive network of hydrogen bonds.

The second group deals with the two-dimensional compounds $[Zn(dmmal)(H_2O)]_n$ (**8**) (H_2dmmal = dimethylmalonic acid, JESSUW) $P2_1/c$), $[Zn(mal)(H_2O)_2]_n$ (**9**) (QQQFQY) ($I2/m$) and $[Zn_2(mal)_2(H_2O)_4]_n$ (**10**) (QQQFQY01) crystallizing in the $P2_1/c$, $I2/m$ and $C2/m$ space groups, respectively; where R-malonate ligand adopts the same bidentate + bis-monodentate coordination mode. The substitution of the two hydrogen atoms of the methylene carbon of the malonate ligand by methyl groups causes significant distortions of this network. The octahedral environment of the zinc(II) ion in these malonate compounds is distorted towards a trigonal bipyramidal polyhedron due to geometrical and steric constraints of the dimethyl group. When the carbon skeleton of the R-malonate is omitted (i.e. only the carboxylate bridges are taken into account), the topology of the layers corresponds to a distorted $[4^4{\cdot}6^2]$ rectangular grid. However, if the R-mal as a whole is considered in the analysis, the topologies vary. So, 3,4-connected binodal 2D network with the Schläfli symbol $[4{\cdot}6^2][4^2{\cdot}6^2{\cdot}8^2]$ is observed for the isostructural compounds **9** and **10**, the R-malonate ligands and the $[Zn(H_2O)_2]^{2+}$ units being the three-fold connectors and the four-fold nodes, respectively, whereas a uninodal $[4{\cdot}8^2]$ net occurs in the dimethylmalonate complex (**8**) (Fig. 5).

The last group is formed by the compound $[Zn(OHcbmal)(H_2O)_2]_n \cdot 2n(H_2O)$ (**11**) (OHcbmal = dianion of the 3-hydroxycyclobutane-1,1-dicarboxylic acid, FUZYOP) crystallizing in the $P2_1/c$ space group. This malonate derivative exhibits the bidentate + bis-monodentate coordination mode towards the zinc(II) as in the previous family, the difference being that here one of the carboxylate-oxygens remains uncoordinated and the hydroxyl group is involved in the coordination. The crystal structure is also two-dimensional as in the precedent cases, but from a topological point of view, this network is completely different from the previous ones. The 2D-net is made up by two topologically identical three-fold nodes, the 3-hydroxycyclobutane-1,1-dicarboxylate ligand and the $[Zn(H_2O)_2]^{2+}$ cations, to form a $[6^3]$ **hcb**-net (Fig. 5).

In contrast with the previous reported compounds, **1** is the first structurally characterized example of zinc(II)-based R-malonate complex with the μ_3-$\kappa^2O{:}\kappa O'{:}\kappa O''{:}\kappa O'''$ coordination mode. As a result, **1** is the first 3D R-malonate/Zn(II) compound without any other co-ligand except the water molecules. This unprecedented coordination mode allows the occurrence of the (10,3)-d or **utp**-net, where two different nodes have been considered, the Memal anions and the $[Zn(H_2O)]^{2+}$ cations acting as a three-fold nodes. There is only one 3D R-malonate transition metal complex, the $\{[Cu(H_2O)_3][Cu(mal)_2]\}_n \cdot 2nH_2O$ (H_2mal = malonic acid) compound that crystallizes in the $Pna2_1$ space group which is indeed reported as a 2D net [34], although it can actually be described as a three-dimensional $[10^3]$ **utp**-net.

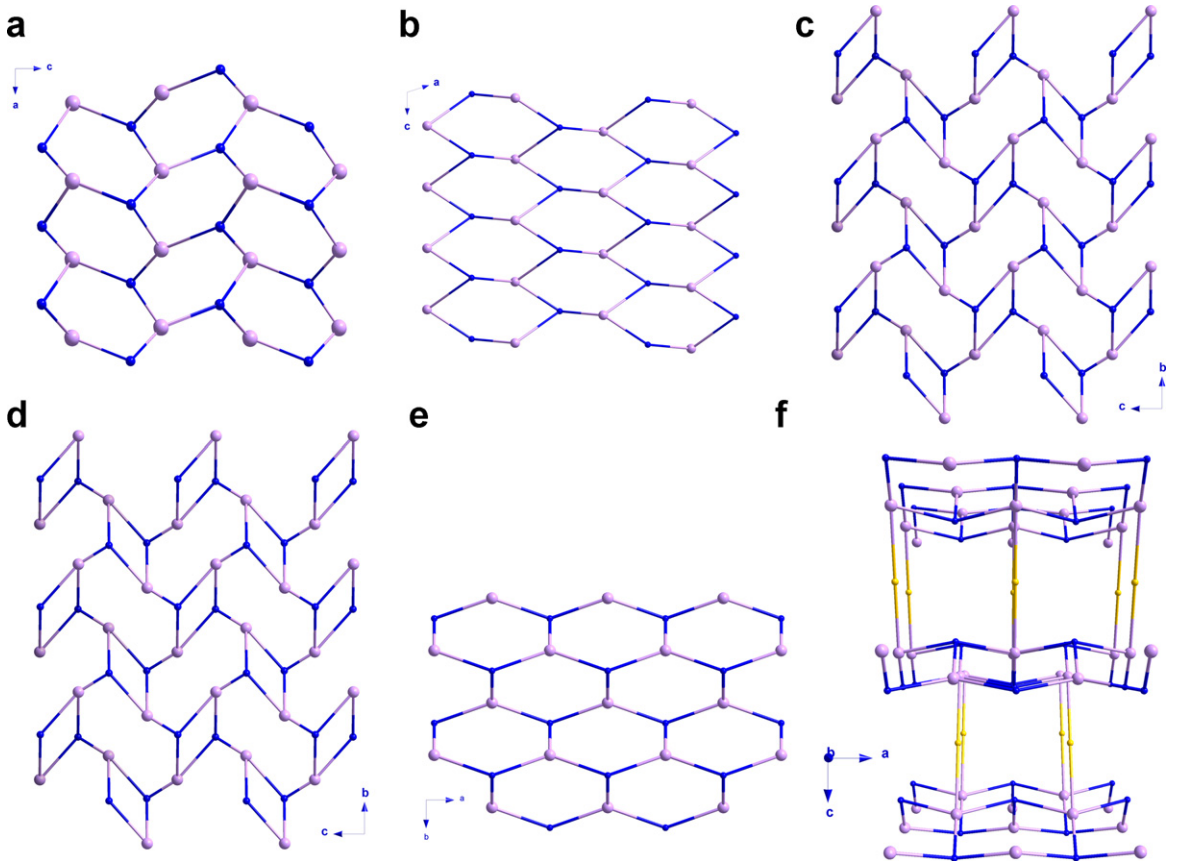

Fig. 5. Topological views of compounds **1** (a) and **8** (b) along the *b* axis and, **10** (c) and **11** (d) along the *a* axis, the honeycomb layers along the *c* axis (e) which are pillared to form the **ins**-network of **2**-**5** viewed along the crystallographic *b* axis (f). The purple balls are the Zn(II) atoms, the blue ones represent the R-malonate ligand and the yellow spheres correspond to the rod-like L co-ligands.

The inclusion of rod-like co-ligands like 4,4′-bpy, bpe, bpa or azpy causes a remarkable change in the crystal structure of $[Zn(Memal)(H_2O)]_n$ (**1**). Its (10,3)-d **utp**-network becomes the 3,4-connected binodal $[6^3][6^5{\cdot}8]$ **ins**-topology (Fig. 5), where the Memal anions and the $[Zn(H_2O)]^{2+}$ units act as three- and four-fold nodes, respectively. The structure is a pillared layered one with the topology of each layer corresponding to a $[6^3]$ **hcb**-net; this hexagonal framework is the same than those observed in the previously published $[Cu(Memal)(H_2O)]_n$ [13a] as well as in other malonate-containing compounds [9,15,16,35]. A detailed scheme with the different topologies discussed above is shown in Fig. 5. Despite the differences in the topologies observed for the R-malonate complexes, the bidentate + bis-monodentate coordination mode of the malonate group being present in most of them, the $[6^3]$ layers are observed in **2**-**5** (Figs. 5 and S4). Nevertheless, the constraints issued from the substitution in the Memal respect to the simpler malonate as shown in **1**, is at the origin of new coordination modes and then, new topologies.

The desired structural role of the extended rod-like ligands in the malonate complexes is to act as connectors between adjacent layers, the separation between the layers being dependent on the co-ligand. This strategy yields interlayer separations ranging from 8.4311(5) to 9.644(3) Å; distances that are shorter than the rod-spacer lengths because of the tilting of the coligand respect to the normal of the $[6^3]$ hexagonal plane [values in the range 45.11(7)°–49.54(3)°]. The cavities formed are large enough to allow two disordered positions or vibration of the N,N′-linkers as it has been observed in **2** and **5**. The free rotation of the pillar modulus is precluded for steric reasons in **2** (Fig. S5), where a methyl group of the Memal ligand blocks the movement of the 4,4′-bpy ligand. The blocking effect of the methyl group in **5** is surprisingly avoided due to the conformation of the azpy ligand, which allows the inclusion of the methyl group in the void space between two pyridyl groups (Fig. S6). Therefore, the rotation of the pyridyl groups of the azpy is now possible. Based on the size and direction of the thermal ellipsoids observed in the X-ray studies, the vibration between two main positions of the pyridyl groups of the 4,4′-bpy ligand in **2** or the free rotation of the azpy ligand in **5** are possible. Further studies to establish the possible amphidynamic behavior of these compounds, in particular for compound **5** that has a sterically unhindered environment, are in progress.

3.3. Thermogravimetric study

The TG curve of the thermal decomposition of $[Zn(Memal)(H_2O)]_n$ (**1**) can be described as a plateau, supporting the lack of solvent molecules of crystallization in the structure of the complex, which is thermally stable up to 220 °C. Then, the degradation process starts with a great weight loss on the TG curve (~65%) in two overlapped steps [$(DTG)_{peaks}$ at 267 and 293 °C] and a strong endothermic effect on the DTA curve with a minimum at 255 °C, which are consistent with the loss of the coordinated water molecules and the final collapse of the lattice structure (vide supra). Further, the degradation continued without formation of any thermally stable intermediate up to 334 °C. Weak exothermic effects with maxima at 330 °C accompanied this part of the thermal decomposition, and it corresponds to the release and pyrolysis of the organic part of the complex. The thermal decay is finished at 334 °C when a solid residue (most likely ZnO) is formed. On the other hand, **2**-**5** show very similar thermogravimetric behaviours which are comparable to that of **1** (Figs. 6 and S7). The thermal behavior of **2**-**5** showed substantially less stability than **1**, being thermally stable up to 170 °C, followed by some complicated overlapped weight losses (Figs. 6 and S7). One endothermic effect with minimum at 207 °C, which might be associated with melting of unstable intermediates, and various exothermic effects with maxima at 250, 317 and 827 °C accompany this part of the decomposition. These latter sharp exothermic effects can be connected with the release and pyrolysis of the organic parts of the complexes.

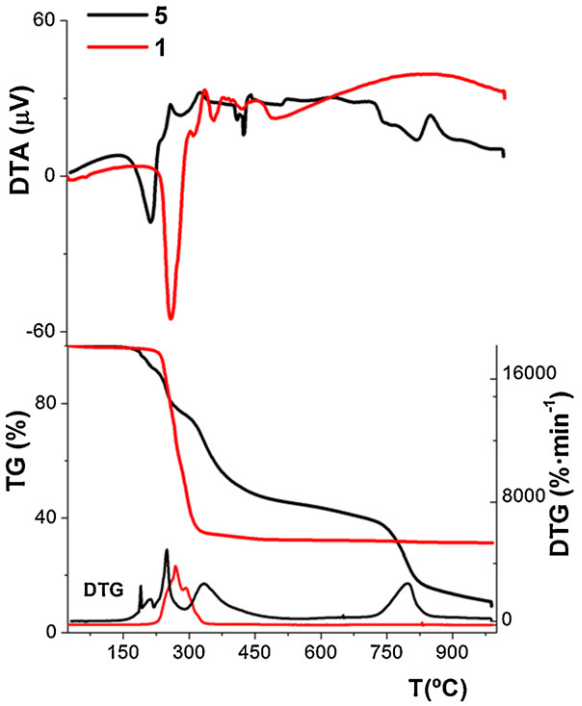

Fig. 6. TG/DTG-DTA curves of **1** (red line) and **5** (black line). TG = mass loss (percent); DTA = ΔT (μV) and DTG = percent per minute (↓ endo and ↑ exo).

3.4. Spectroscopic studies

Metal-organic compounds that combine d^{10} metal ions, such as Zn^{2+} in methylmalonate centers with conjugated monomers acting as ligand units, are interesting structures to control, modify the luminescence properties of the fluorescent conjugated monomers, and in the case of crystallization in polar space groups, as in **1**, it can lead to NLO effects [13d,36]. The room temperature steady-state fluorescence emission spectra of the isolated 4,4′-bpy, bpe, bpa and azpy ligands are reported in Fig. 7. They show broad emission bands centered at 555, 525, 467, and 550 nm, for the 4,4′-bpy, bpe, bpa and azpy ligands, respectively. It is worth noting that the intensity of the emission of the azpy ligand was several orders of magnitude lower than the other ones. The electronegative azo group in the azpy ligand will most likely reduce the delocalization of the π electrons of the aromatic rings and, consequently, decreases the radiative emission probability.

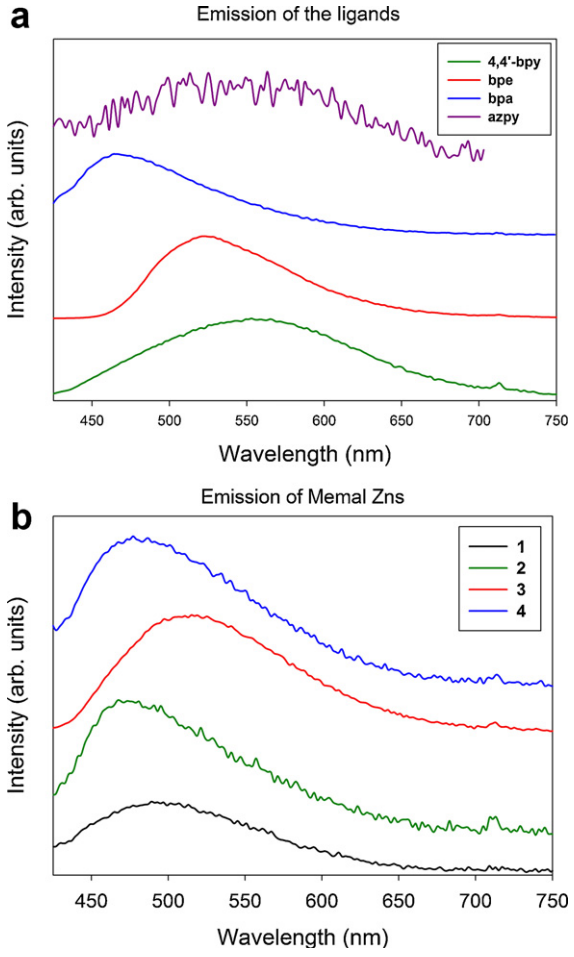

Fig. 7. Solid-state fluorescence emission spectra of the isolated four L co-ligands (a), and of the four fluorescent metal-organic compounds **1**-**4** (b).

The emission spectra of **1**-**4** are presented in the Fig. 7. The pump wavelength was 405 nm in all cases, which corresponds to the low energy tail of the absorption band of the compounds. Interestingly, the compound **1**, the Zn(II)-metylmalonate complex with water molecules as unique coligands, shows a fluorescent band centered at 490 nm. The physical origin of this emission could be related to luminescent defects on the structure; further investigations would be necessary to clarify this issue. The position of the emission bands for compound **2**, **3** and **4** are ca. 475, 515, and 477 nm, respectively. The fluorescence of compound **5** was too weak to be detected within our experimental setup, owing to the mentioned low intensity of the azpy ligand. The peak positions of **2** and **3** are blue shifted by 80 and 10 nm compared to the emission of the isolated ligands, which might be assigned to intraligand transitions [37].

On the contrary, the position of the emission band of **4** is red shifted by about 10 nm. The blue or red shifts are due to metal-ligand coordination interactions. In order to determine the effect of this interaction on the radiative relaxation probability, the decay of the fluorescence of the isolated ligands and the resulting complexes have been measured and they are reported in Fig. 8. The decay curves

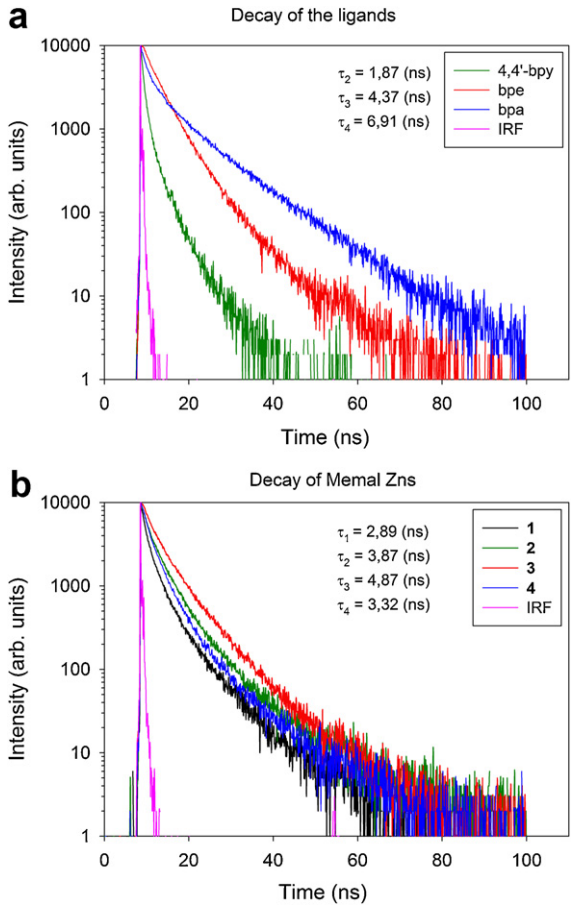

Fig. 8. Decay of the fluorescence of the isolated co-ligands bpe, bpa and azpy (a), and of the compounds **1**-**4** (b) (see text). The instrumental response function is included for comparison.

are not exponential, which is rather common in organic compounds where a distribution of environments might be present. The experimental decays have been fitted to a two exponential decay curve of the form:

$$I(t) = a_1 \exp\left(-t/\tau_1\right) + a_2 \exp\left(-t/\tau_2\right)$$

where a_1 and a_2 are pre-exponential factors and τ_1 and τ_2 are the corresponding decay constants. The average lifetime is then defined as [38]:

$$(\tau) = \left(a_1\tau_1^2 + a_2\tau_2^2\right) / \left(a_1\tau_1 + a_2\tau_2\right)$$

The average lifetime values obtained from the best-fits of the curves of the isolated ligands were 1.9, 4.4, and 6.9 ns for 4,4′-bpy, bpe and bpa, respectively. The intensity of the emission of the azpy ligand was not strong enough to determine its decay curve. The average lifetimes for compounds **1**-**4** were 2.9, 3.9, 4.9 and 3.3 ns. It is remarkable that the metylmalonate complex without coligand showed a shorter lifetime than the other compounds, which might be due to more non-radiative relaxation processes when the metal center is not coordinated to aromatic coligands.

A comparison between the coligands and the associated complexes shows an increase of the lifetime in compounds **2** and **3** as related to their respective coligands. On the other hand, the lifetime of **4** is much smaller than that of the isolated bpa ligand. It seems that the blue shift effect due to metal-ligand interactions in compounds **2** and **3** tends to reduce possible energy loss mechanisms, increasing, therefore, the lifetime. Furthermore, the increase of the lifetime is more significant in compound **2**, where the blue shift was more important. On the contrary, the red shift observed for **4** seems to be associated with a decrease of lifetime, which could be due to new non-radiative relaxation processes via metal-ligand interactions. All these data seem to indicate that there are electronic interactions between the metal centre and the aromatic coligands in **2**-**4**. This interaction can increase or decrease the radiative quantum yield of the complex depending on the specific characteristic of each ligand.

4. Conclusion

Three main points can be outlined from this work:

- the [10^3] **utp** 3D crystal structure of [Zn(Memal)(H_2O)]$_n$ (**1**) is completely changed under the presence of a rod-like spacer in the preparative process as illustrated by compounds **2**-**5**. However, the Memal still acts as a three-fold connector leading to a [6^3] **hcb**-layer, which is then pillared by the rigid co-ligand;
- the **utp**-net of **1** is non-centrosymmetric, a remarkable situation since all its components are achiral. The corresponding malonate-containing zinc(II) complexes are centrosymmetric, as the dimethylmalonate ones. Therefore, we guess that the substitution of one methylene-hydrogen atom of the malonate by a group like the methyl one produces an asymmetry in the Memal ligand capable of forming chiral architectures. This assertion is supported by the reported chiral

structure of the Mn(II)-Etmal (crystallizing in the $C222_1$ space group), but it should be further investigated;
- metal-ligand interactions influence the fluorescent properties of the resulting complex. The radiative quantum yield of the fluorescent ligands can increase due to their interaction with the metal centre. Further work is in progress to determine and optimize the quantum yields of the metal-organic complexes and it will be published elsewhere.

Finally, our results show that the rational design to obtain a predictable conformation is a very difficult task: chemical affinity, coordination modes of the ligands, as well as weak interactions must be controlled very carefully and systematic studies are mandatory to significantly advance progress in this research area.

Acknowledgements

Funding for this work provided by the Ministerio de Ciencia e Innovación through the projects MAT2010-16981, Consolider Ingenio2010–CSD2006-0015, DPI2010-21103-C04-03 and by the Agencia Canaria de Investigación, Innovación y Sociedad de la Información, Gobierno de Canarias through projects PIL2070901, SolSubC200801000088 and structuring NANOMAC is gratefully acknowledged. M.D. thanks the Spanish Ministerio de Educación y Cultura for a predoctoral fellowship. J.P. also thanks the NANOMAC project of the ACIISI for a postdoctoral contract.

Appendix A. Supplementary data

Supplementary data associated with this article can be found, in the online version, at http://dx.doi.org/10.1016/j.crci.2012.04.007. The crystal packing of complexes **2**, **3** and **5**, together with the honeycomb carboxylate-bridged zinc(II) network of **2**-**5** are shown in Figs. S1–S4. Figs. S5 and S6 show the packing around the disordered 4,4′-bpy and azpy co-ligands in **2** and **5**, respectively. The thermogravimetric curves of complexes **2**-**4** are depicted on Fig. S7.

CCDC reference numbers 869333, 869334, 869335 and 869336 contain de supplementary crystallographic data for **1**, **3**-**5**, respectively. These data can be obtained free of charge via http://www.ccdc.cam.ac.uk/conts/retrieving.html, or from the Cambridge Crystallographic Data Centre, 12, Union Road, Cambridge CB2 1EZ, UK; fax: +44 1223 336 033; e-mail: deposit@ccdc.cam.ac.uk.

References

[1] (a) S.L. Stupp, P.V. Braun, Science 277 (1997) 1242;
(b) S. Kitagawa, R. Kitaura, S. Noro, Angew. Chem. Int. Ed. 43 (2004) 2334;
(c) G. Ferey, Chem. Soc. Rev. 37 (2008) 191.
[2] (a) C. Janiak, Dalton Trans. (2003) 2781;
(b) J. Lee, O.K. Fartha, J. Roberts, K.A. Scheidt, S.T. Nguyen, J.T. Hupp, Chem. Soc. Rev. 38 (2009) 1450;
(c) M.D. Allendorf, C.A. Bauer, R.K. Bhakta, R.J.T. Houk, Chem. Soc. Rev. 38 (2009) 1330;
(d) M. Kurmoo, Chem. Soc. Rev. 38 (2009) 1353.
[3] (a) L. Brammer, Chem. Soc. Rev. 33 (2004) 476;
(b) K. Biradha, C.-Y. Su, J.J. Vittal, Cryst. Growth Des. 11 (2011) 875;
(c) M. Nakash, Z. Clyde-Watson, N. Feeder, S.J. Teat, J.K.M. Sanders, Chem. Eur. J. 6 (2000) 2112;
(d) A.J. Dobson, R.E. Gerkin, Acta Cryst. C54I (1998) 1503.
[4] (a) T.M. Reineke, M. Eddaoudi, M. O'Keeffe, O.M. Yaghi, Angew. Chem. Int. Ed. 38 (1999) 2590;
(b) M. Eddaoudi, D.B. Moler, H.L. Li, B.L. Chen, T.M. Reineke, M. O'Keeffe, O.M. Yaghi, Acc. Chem. Res. 34 (2001) 319;
(c) D. Bradshaw, J.B. Claridge, E.J. Cussen, T.J. Prior, M.J. Rosseinsky, Acc. Chem. Res. 38 (2005) 273.
[5] (a) W. Mori, S. Takamizawa, J. Solid State Chem. 152 (2000) 120;
(b) L. Pan, N. Ching, X.Y. Huang, J. Li, Inorg. Chem. 39 (2000) 5333;
(c) L. Pan, B.S. Finkel, X.Y. Huang, J. Li, Chem. Commun. (2001) 105.
[6] (a) N.L. Rosi, M. Eddaoudi, J. Kim, M. O'Keeffe, O.M. Yaghi, Angew. Chem. Int. Ed. 41 (2002) 284;
(b) L.M. Zheng, T. Whitfield, X.Q. Wang, A.J. Jacobson, Angew. Chem. Int. Ed. 39 (2000) 4528;
(c) O.R. Evans, W.B. Lin, Acc. Chem. Res. 35 (2002) 511.
[7] C.N.R. Rao, S. Natarajan, R. Vaidhyanathan, Angew. Chem. Int. 43 (2004) 1466.
[8] (a) C. Ruiz-Pérez, P.A. Lorenzo-Luis, M. Hernández-Molina, M.M. Laz, P. Gili, M. Julve, Cryst. Growth Des. 4 (2004) 57;
(b) F.S. Delgado, J. Sanchiz, C. Ruiz-Pérez, F. Lloret, M. Julve, Cryst. Eng. Comm. 5 (2003) 280.
[9] (a) Pillared Layered Structures: Current Trends and Applications, ed. I. V. Mitchell, Elsevier, London, 1990;
(b) N.L. Rosi, J. Kim, M. Eddaoudi, B.L. Chen, M. O'Keeffe, O.M. Yaghi, J. Am. Chem. Soc. 127 (2005) 1504.
[10] (a) R.W. Gable, B.F. Hoskins, R. Robson, Chem. Commun. (1990) 1677;
(b) L. Carlucci, G. Ciani, D.M. Proserpio, A. Sironi, Inorg. Chem. 34 (1995) 5698;
(c) S. Sibramanian, M.J. Zaworotko, Angew. Chem. Int. Ed. 34 (1995) 2127;
(d) F. Lloret, G. De Munno, M. Julve, J. Cano, R. Ruiz, A. Caneschi, Angew. Chem. Int. Ed. 37 (1998) 135;
(e) A.J. Blake, N.R. Champness, M. Crew, L.R. Hanton, S. Parsons, M. Schröder, Dalton Trans. (1998) 1533.
[11] (a) S.R. Batten, R. Robson, Angew. Chem. Int. Ed. 37 (1998) 1461;
(b) S.R. Batten, Cryst. Eng. Comm. 3 (2001) 67;
(c) S.L. James, Chem. Soc. Rev. 32 (2003) 276;
(d) S. Noro, R. Kitamura, M. Kondo, S. Kitagawa, T. Ishii, H. Matsuzaka, M. Yamashita, J. Am. Chem. Soc. 124 (2002) 2568;
(e) J. Tao, M.L. Tong, X.M. Chen, Dalton Trans. (2000) 3669.
[12] C.B. Aakeröy, N.R. Champness, C. Janiak, Cryst. Eng. Comm. 12 (2010) 22.
[13] (a) J. Pasán, J. Sanchiz, F. Lloret, M. Julve, C. Ruiz-Pérez, Cryst. Eng. Comm. 9 (2007) 478;
(b) H.A. Habib, J. Sanchiz, C. Janiak, Inorg. Chim. Acta 362 (2009) 2452;
(c) H.A. Habib, A. Hoffmann, H.A. Höppe, C. Janiak, Dalton Trans. (2009) 1742;
(d) H.A. Habib, J. Sanchiz, C. Janiak, Dalton Trans. (2008) 1734;
(e) B. Wisser, Y. Lu, C. Janiak, Z. Anorg. Allg. Chem. 633 (2007) 1189.
[14] (a) J. Pasán, F.S. Delgado, Y. Rodríguez-Martín, M. Hernández-Molina, C. Ruiz-Pérez, J. Sanchiz, F. Lloret, M. Julve, Polyhedron 22 (2003) 2143;
(b) Y. Rodríguez-Martín, M. Hernández-Molina, F.S. Delgado, J. Pasán, C. Ruiz-Pérez, J. Sanchiz, F. Lloret, M. Julve, Cryst. Eng. Comm. (2002) 522;
(c) C. Ruiz-Pérez, Y. Rodríguez-Martín, M. Hernández-Molina, F.S. Delgado, J. Pasán, J. Sanchiz, F. Lloret, M. Julve, Polyhedron 22 (2003) 2111;
(d) F.S. Delgado, F. Lahoz, F. Lloret, M. Julve, C. Ruiz-Pérez, Cryst. Growth Des. 8 (2008) 3219.
[15] (a) J. Pasán, J. Sanchiz, C. Ruiz-Pérez, F. Lloret, M. Julve, New J. Chem. 27 (2003) 1557;
(b) J. Pasán, J. Sanchiz, C. Ruiz-Pérez, F. Lloret, M. Julve, Eur. J. Inorg. Chem. (2004) 4081;
(c) J. Pasán, J. Sanchiz, C. Ruiz-Pérez, F. Lloret, M. Julve, Inorg. Chem. 44 (2005) 7794;
(d) J. Pasán, J. Sanchiz, C. Ruiz-Pérez, J. Campo, F. Lloret, M. Julve, Chem. Commun. (2006) 2857.
[16] (a) M. Déniz, J. Pasán, O. Fabelo, L. Cañadillas-Delgado, F. Lloret, M. Julve, C. Ruiz-Pérez, New J. Chem. 34 (2010) 2515;
(b) J. Pasán, J. Sanchiz, L. Cañadillas-Delgado, O. Fabelo, M. Déniz, F. Lloret, M. Julve, C. Ruiz-Pérez, Polyhedron 28 (2009) 1802.
[17] A. Erxleben, Coord. Chem. Rev. 246 (2003) 203.
[18] (a) K.-L. Zhang, H.-W. Kuai, G.-W. Diao, J. Mol. Struct. 779 (2005) 11;
(b) C.-X. Meng, X.-G. Zheng, F. Fu, X.-N. Zhang, P. Zhang, Acta Cryst. Sect. E 65 (2009) m1604;
(c) Y.-G. Sun, L. Ren, E.-J. Gao, X. Liu, C.-S. Wang, Acta Cryst. Sect. E 62 (2006) m2578;
(d) X.-C. Fu, M.-T. Li, C.-G. Wang, Acta Cryst. Sect. C 62 (2006) m13;
(e) D.K. Kumar, Inorg. Chim. Acta 362 (2009) 1767;

(f) Y.-M. Chen, Q.-F. Xie, Acta Cryst. Sect. E 67 (2011) m66;
(g) M. Hemamalini, P.T. Muthiah, R.J. Butcher, D.E. Lynch, Inorg. Chem. Commun. 9 (2006) 1155;
(h) B.-X. Liu, G.-H. Chen, Y.-P. Yu, Y.-Y. Li, Acta Cryst. Sect. E 63 (2007) m2054;
(i) D.J. Darensbourg, M.W. Holtcamp, B. Khandelwal, K.K. Klausmeyer, J.H. Reibenspies, Inorg. Chem. 34 (1995) 2389.
[19] (a) A.D. Burrows, R.W. Harrington, M.F. Mahon, C.E. Price, Dalton Trans. (2000) 3845;
(b) F.S. Delgado, J. Sanchiz, C. Ruiz-Pérez, F. Lloret, M. Julve, Cryst. Eng. Comm. 5 (2003) 280;
(c) A.D. Burrows, A.S. Donovan, R.W. Harrington, M.F. Mahon, Eur. J. Inorg. Chem. (2004) 4686;
(d) Y. Ling, L. Zhang, J. Li, A.X. Hu, Cryst. Growth Des. 9 (2009) 2043;
(e) W. Zhao, J. Fan, T. Okamura, W.-Y. Sun, N. Ueyama, J. Solid State Chem. 177 (2004) 2358;
(f) A.D. Burrows, R.W. Harrington, M.F. Mahon, S.J. Teat, Cryst. Eng. Comm. 7 (2005) 388;
(g) Q. Liu, Y.-Z. Li, Y. Song, H. Liu, Z. Xu, J. Solid State Chem. 177 (2004) 4701;
(h) Y. Zhang, J. Li, J. Chen, Q. Su, W. Deng, M. Nishiura, T. Imamoto, X. Wu, Q. Wang, Inorg. Chem. 39 (2000) 2330;
(i) T. Basu, H.A. Sparkes, M.K. Bhunia, R. Mondal, Cryst. Growth Des. 9 (2009) 3488;
(j) T. Ni, F. Xing, M. Shao, Y. Zhao, S. Zhu, M. Li, Cryst. Growth Des. 11 (2011) 2999;
(k) G.A. Farnum, J.H. Nettleman, R.L. LaDuca, Cryst. Eng. Comm. 12 (2010) 888.
[20] (a) M.-L. Guo, Y.-N. Zhao, Acta Cryst. Sect. C 62 (2006) m563;
(b) L. Walter-Levy, J. Perrotey, J.W. Visser, C. R. Acad. Sci. Ser. C (Chim) 277 (1973) 1351;
(c) N.J. Ray, B.J. Hathaway, Acta Cryst. Sect. B 38 (1982) 770;
(d) U.C. Sinha, S. Ojha, Z. Kristallogr 152 (1980) 157;
(e) X.-Z. Chen, Q.-S. Ye, M.-J. Xie, J.-L. Chen, Z.-F. Pan, X.-H. Yang, W.-P. Liu, Z. Kistrallogr. New Cryst. Struct. 225 (2010) 517.
[21] (a) E.V. Brown, G.R. Granneman, J. Am. Chem. Soc. 97 (1975) 621;
(b) A. Kirpal, E. Reiter, Chem. Ber. 60 (1927) 664;
(c) A. Kirpal, Chem. Ber. 67 (1934) 70;
(d) J.P. Launay, M. Tourrel-Pagis, J.-F. Lipskier, V. Marvaud, C. Joachim, Inorg. Chem. 30 (1991) 1033.
[22] G.M. Sheldrick, Acta Cryst. D66I (2010) 479.
[23] L.J. Farrugia, (WINGX) J. Appl. Cryst. 32 (1999) 837.
[24] A.L. Spek, Acta Cryst. D65I (2009) 148.
[25] (a) H.D. Flack, M. Sadki, A.L. Thompson, D.J. Watkin, Acta Crystallogr. Sect. A 67 (2011) 21;
(b) H.D. Flack, G. Bernardinelli, Chirality 20 (2008) 681;
(c) H.D. Flack, G. Bernardinelli, Acta Crystallogr. Sect. A 55 (1999) 908.
[26] M. O'Keeffe, M.A. Peskov, S.J. Ramsden, O.M. Yaghi, Acc. Chem. Res. 41 (2008) 1782.
[27] (a) S.R. Halper, S.M. Cohen, Inorg. Chem. 44 (2005) 486;
(b) L. Öhrström, K. Larsson, S. Borg, S.T. Norberg, Chem. Eur. J. 7 (2001) 4805;
(c) Y.B. Dong, M.D. Smith, H.C. zur Loye, Inorg. Chem. 39 (2000) 4927.
[28] (a) A.A. Massoud, A. Hefnawy, V. Langer, M.A. Khatab, L. Öhrstrom, M.A.M. Abu-Youssef, Polyhedron 28 (2009) 2794;
(b) C.A. Black, L.R. Hanton, Cryst. Growth Des. 7 (2007) 1868;
(c) J. Zhang, Y.-B. Chen, S.-M. Chen, Z.-J. Li, J.-K. Cheng, Y.-G. Yao, Inorg. Chem. 45 (2006) 3161.
[29] (a) B. Gil-Hernández, H.A. Höppe, J.K. Vieth, J. Sanchiz, C. Janiak, Chem. Commun. 46 (2010) 8270;
(b) A.C. Chamayou, M.A. Neelakantan, S. Thalamuthu, C. Janiak, Inorg. Chim. Acta 365 (2011) 447;
(c) C. Janiak, A.C. Chamayou, A.K. Royhan Uddin, M. Uddin, K.S. Hagen, M. Enamullah, Dalton Trans. (2009) 3698;
(d) M. Enamullah, A. Sarmin, M. Hasegawa, T. Hoshi, A.C. Chamayou, C. Janiak, Eur. J. Inorg. Chem. (2006) 2146.
[30] E.I. Stiefel, G.F. Brown, Inorg. Chem. 11 (1972) 434.
[31] A.W. Addison, T.N. Rao, J. Reedijk, J. van Rijn, G.C. Verschoor, Dalton Trans. (1984) 1349.
[32] (a) L. Carlucci, G. Ciani, D.W. van Gudenberg, D.M. Proserpio, A. Sironi, Chem. Commun. (1997) 631;
(b) J.-D. Lin, J.-W. Chen, H.-S. Weng, S.-W. Du, Inorg. Chem. Commun. 11 (2008) 1136;
(c) S.-S. Chen, J. Fan, T. Okamura, M.-S. Chen, Z. Su, W.-Y. Sun, N. Ueyama, Cryst. Growth Des. 10 (2010) 812;
(d) A.M. Kirillov, S.W. Wieczorek, M.F.C.G. da Silva, J. Sokolnicki, P. Smolenski, A.J.L. Pombeiro, Cryst. Eng. Comm. 13 (2011) 6329;
(e) A.C. Kathalikkattil, K.K. Bisht, N. Aliaga-Alcaide, E. Suresh, Cryst. Growth Des. 11 (2011) 1631.
[33] C. Janiak, Dalton Trans. (2000) 3885.
[34] V.T. Yilmaz, E. Senel, Trans. Metal Chem. 29 (2004) 336.
[35] (a) Y. Rodríguez-Martín, M. Hernández-Molina, J. Sanchiz, C. Ruiz-Pérez, F. Lloret, M. Julve, Dalton Trans. (2003) 2359;
(b) S. Konar, P.S. Mukherjee, M.G.B. Drew, J. Ribas, N.R. Chaudhuri, Inorg. Chem. 42 (2003) 2545;
(c) R. Baldoma, M. Monfort, J. Ribas, X. Solans, M.A. Maestro, Inorg. Chem. 45 (2006) 8144;
(d) M.R. Montney, R.M. Supkowsky, R.L. LaDuca, Polyhedron 27 (2008) 2997.
[36] (a) C. Janiak, T.G. Scharmann, P. Albrecht, F. Marlow, R. Macdonald, J. Am. Chem. Soc. 118 (1996) 6307;
(b) H.A. Habib, A. Hoffmann, H.A. Höppe, G. Steinfeld, C. Janiak, Inorg. Chem. 48 (2009) 2166;
(c) S. Zang, Y. Su, Y.Z. Li, J. Lin, X. Duan, Q. Meng, S. Gao, Cryst. Eng. Comm. 11 (2009) 122;
(d) P. Ren, M.L. Liu, J. Zhang, W. Shi, P. Cheng, D.Z. Liao, S.P. Yan, Dalton Trans. (2008) 4711;
(e) W. Liu, L. Ye, X. Liu, L. Yuan, J. Jiang, C. Yan, Cryst. Eng. Comm. 10 (2008) 1395.
[37] (a) D.R. Xiao, Y.G. Li, E.B. Wang, L.L. Fan, H.Y. An, Z.M. Su, L. Xu, Inorg. Chem. 46 (2007) 4158;
(b) A. Vogler, H. Kunkely, Coord. Chem. Rev. 250 (2006) 1622;
(c) Z.-H. Yang, X.-F. Xiong, H.-M. Hu, Y. Luo, L.-H. Zhang, Q.-H. Bao, Y.-Q. Shang-Guan, G.-L. Xue, Inorg. Chem. Commun. 14 (2011) 1406.
[38] J.R. Lakowicz, Principles of Fluorescence Spectroscopy, Springer, 2010.